Feasibility of ^{18}F-FDG Dose Reductions in Breast Cancer PET/MRI

Bert-Ram Sah[1–4], Soleen Ghafoor[3,4], Irene A. Burger[1,4,5], Edwin E.G.W. ter Voert[1,4], Tetsuro Sekine[1], Gaspar Delso[1,6], Martin Huellner[1,4], Konstantin J. Dedes[5,7], Andreas Boss[3,4], and Patrick Veit-Haibach[1,3,4,8,9]

[1]Department of Nuclear Medicine, University Hospital of Zurich, Zurich, Switzerland; [2]Department of Cancer Imaging, King's College London, London, United Kingdom; [3]Department of Diagnostic and Interventional Radiology, University Hospital of Zurich, Zurich, Switzerland; [4]University of Zurich, Zurich, Switzerland; [5]Cancer Center Zurich, Zurich, Switzerland; [6]GE Healthcare, Waukesha, Wisconsin; [7]Department of Gynaecology, University Hospital of Zurich, Zurich, Switzerland; [8]Joint Department of Medical Imaging, University Health Network, Toronto, Ontario, Canada; and [9]University of Toronto, Toronto, Ontario, Canada

The goal of this study was to determine the level of clinically acceptable ^{18}F-FDG dose reduction in time-of-flight PET/MRI in patients with breast cancer. **Methods:** Twenty-six consecutive women with histologically proven breast cancer were analyzed (median age, 51 y; range, 34–83 y). Simulated dose-reduced PET images were generated by unlisting the list-mode data on PET/MRI. The acquired 20-min PET frame was reconstructed in 5 ways: a reconstruction of the first 2 min with 3 iterations and 28 subsets for reference, and reconstructions simulating 100%, 20%, 10%, and 5% of the original dose. General image quality and artifacts, image sharpness, image noise, and lesion detectability were analyzed using a 4-point scale. Qualitative parameters were compared using the nonparametric Friedman test for multiple samples and the Wilcoxon signed-rank test for paired samples. Different groups of independent samples were compared using the Mann–Whitney *U* test. **Results:** Overall, 355 lesions (71 lesions with 5 different reconstructions each) were evaluated. The 20-min reconstruction with 100% injected dose showed the best results in all categories. For general image quality and artifacts, image sharpness, and noise, the reconstructions with a simulated dose of 20% and 10% were significantly better than the 2-min reconstructions ($P \leq 0.001$). Furthermore, 20%, 10%, and 5% reconstructions did not yield results different from those of the 2-min reconstruction for detectability of the primary lesion. For 10% of the injected dose, a calculated mean dose of 22.6 ± 5.5 MBq (range, 17.9–36.9 MBq) would have been applied, resulting in an estimated whole-body radiation burden of 0.5 ± 0.1 mSv (range, 0.4–0.7 mSv). **Conclusion:** Ten percent of the standard dose of ^{18}F-FDG (reduction of ≤90%) results in clinically acceptable PET image quality in time-of-flight PET/MRI. The calculated radiation exposure would be comparable to the effective dose of a single digital mammogram. A reduction of radiation burden to this level might justify partial-body examinations with PET/MRI for dedicated indications.

Key Words: dose reduction; positron emission tomography; magnetic resonance; image reconstruction; breast cancer

J Nucl Med 2018; 59:1817–1822
DOI: 10.2967/jnumed.118.209007

PET/CT is one of the most widely used hybrid imaging tools for staging, therapy response assessment, and follow-up of different malignant diseases (*1,2*). In PET/CT, the CT component is used for attenuation correction and for anatomic correlation and characterization of neoplastic lesions, whereas the PET component is used to identify lesions with increased radiotracer uptake (*3,4*). In breast cancer, clinical PET/CT has been used mainly as a whole-body examination for disease detection, therapy follow-up, and response assessment, as well as for prognostic stratification (*5*). Despite promising results with PET mammography (PEM), the predominant diagnostic imaging tools for local staging are conventional mammography, ultrasound, and MRI (*6–8*).

For several years, PET/MRI has been used clinically and scientifically for the evaluation of several neoplastic diseases (*9,10*). In such systems, the MRI component replaces the CT component for attenuation correction and anatomic reference. Because the MRI component is known to have a much higher soft-tissue contrast and because MRI can provide additional information (e.g., diffusivity, intravoxel incoherent motion, iron load, and blood oxygenation level–dependent effect), PET/MRI is expected to have an even greater impact than PET/CT on diagnostic and therapeutic decisions in certain oncologic patients—which remains to be proven (*9,11–14*).

In breast cancer, MRI is mainly used for detection, characterization, and biopsy guidance of lesions but is also partially used for screening (*15*). Nonetheless, like every imaging modality, MRI has its technically inherent limitations. Alternatively, PEM has already been proven to be helpful in characterizing small breast lesions (*16*). However, PEM scanners are specialized systems that cannot be used for a broader range of imaging, and they are not widely available yet. Another argument constantly confronting PET imaging is exposure of the patient to radiation, especially in breast imaging.

New PET technologies used in PET/MRI have been shown to reduce the radiation burden significantly (*17*), and the PET component of the latest clinical time-of-flight (TOF) PET/MRI system has the potential to reduce radiation exposure even further, especially in single-station imaging. This system uses a new PET detector based on silicon photomultipliers (SiPMs) that offer increased sensitivity compared with conventional PET/CT and PET/MRI scanners, allowing the user to balance dose reduction with acquisition time (*18*).

In our study, we evaluated and compared the overall quality, artifacts, sharpness, noise, and lesion detectability of PET/MRI breast cancer images acquired with simulated reduced ^{18}F-FDG

Received Jan. 30, 2018; revision accepted Apr. 27, 2018.
For correspondence or reprints contact: Bert-Ram Sah, Department of Nuclear Medicine, Department of Diagnostic and Interventional Radiology, University Hospital of Zurich, Raemistrasse 100, CH-8091 Zurich, Switzerland.
E-mail: bert-ram.sah@usz.ch
Published online Jun. 7, 2018.

doses. We used a 2-min (per bed position) acquisition as a standard of reference, because this acquisition time is widely used in standard clinical care.

The goal of this study was to determine the acceptable level of ^{18}F-FDG dose reduction in TOF PET/MRI using a SiPM PET detector for breast cancer assessment.

MATERIALS AND METHODS

Ethics Approval and Consent to Participate

All procedures performed in studies involving human participants were in accordance with the ethical standards of the institutional or national research committee and with the 1964 Helsinki declaration and its later amendments or comparable ethical standards. The institutional review board approved this study. Patients were enrolled prospectively as part of a larger study with several different subgroups (KEK-ZH number 2014-0072/NCT02316431). All patients gave written informed consent before being included in the study. There was financial support for this study from GE Healthcare on an institutional level, and an employee of GE Healthcare participated in this study as an author. Only non–GE Healthcare employees had control of inclusion of the data and information that might present a conflict of interest.

Patients

Patients had to meet the following criterion for inclusion in our study: referral for clinical (based on local clinical guidelines) PET/CT for initial staging of histologically confirmed breast cancer. Additionally, the patient needed to be willing to undergo the additional scientific PET/MRI examination of the breast. Exclusion criteria were contraindications to MRI, such as electronically active implanted medical devices, metallic foreign bodies in sensitive anatomic areas (e.g., orbita), severe claustrophobia, or a body size that did not fit into the PET/MRI bore.

Imaging

Patients fasted at least 4 h before injection of the tracer. Patients were injected intravenously with 3 MBq of ^{18}F-FDG per kilogram of body weight if they weighed 85 kg or less and 3.5 MBq/kg otherwise. Clinical PET/CT was performed about 1 h after tracer administration. Patients were injected only once with ^{18}F-FDG; no additional injection was done for the PET/MRI. The mean uptake time (±SD) for the 20-min PET frame was 34 ± 6 min.

The PET/CT acquisition followed our standard protocol for clinical oncologic imaging on a TOF PET/CT scanner as previously published (Discovery 690; GE Healthcare) (*19,20*). The PET/MR system is located in a room adjacent to the PET/CT room; thus, the mean time between the start of the acquisitions was 38 ± 3.5 min.

PET/MRI Acquisition. PET/MRI was performed on a simultaneous TOF PET/MRI scanner (Signa PET/MR; GE Healthcare). Patients were positioned prone on an 8-channel breast coil (GE Healthcare). The coil has a fixed position on the bed, allowing it to be automatically included in the PET attenuation correction.

The PET transaxial field of view is 60 cm, and the axial field of view is 25 cm, allowing the area of interest to be scanned within a single PET bed position (*21*). The per-crystal TOF timing resolution is less than 400 ps (*22*), enabling TOF imaging. PET list-mode data were acquired in 3-dimensional TOF mode with a scan duration of 20 min in the breast bed-position. An axial field of view of 25 cm was used. The time for the PET scan was adapted on the basis of the MRI protocol needed for a dedicated breast MRI examination.

During PET/MR scanning, a default (Dixon-based) MRI acquisition for attenuation correction was performed. Additionally, a dedicated breast MRI protocol was acquired for diagnostic purposes (technical details are provided in Supplemental Table 1; supplemental materials are available at http://jnm.snmjournals.org).

Image Processing. For each patient, the 20-min PET frame was reconstructed into 5 different sets: a reconstruction of the first 2 min with 3 iterations and 28 subsets for reference and comparison (2 min), followed by reconstructions simulating 100%, 20%, 10%, and 5% of the original ^{18}F-FDG dose injected for the clinical PET/CT, all with a 20-min acquisition time. These percentages were based on a preevaluation in which image quality parameters on higher percentages did not show significant differences from the standard of reference. The 100% and 20% datasets were reconstructed with 3 iterations and 28 subsets, and the 10% and 5% datasets were reconstructed with 50 iterations and 1 subset. The different reconstructions were chosen to reflect the differences in counts per reconstruction (the fewer the counts, the fewer are the subsets needed to avoid excessive noise).

Reduction of injected ^{18}F-FDG was simulated by removing the required number of counts from the list-mode data. This removal was performed randomly on a microsecond-by-microsecond basis (with an in-house Matlab script).

In this way, the total scan time remained 20 min and, as a result, the data still included normal effects such as decay, biodistribution, and eventual patient motion. The PET images were reconstructed using the system's default 3-dimensional ordered-subsets expectation-maximization iterative algorithm, which includes all default corrections and incorporates TOF information. The image grid was 256 × 256 pixels, and images were filtered in image space using an in-plane gaussian filter of 4 mm in full width at half maximum followed by an axial filter with a 3-slice kernel using relative weights of 1:4:1.

Image Evaluation. In total, 130 reconstructed PET datasets (26 patient studies with 5 different reconstructions each) were evaluated in consensus by 2 experienced nuclear medicine physician/radiologists (with 5 [reader 1] and 6 y [reader 2] of experience interpreting PET and MRI). These readers were aware of the clinical background of the study but masked to the reconstruction method. For further analysis, lesions were grouped according to their location (primary breast lesions, lymph nodes, and distant metastases). Lesions were selected independently of their size. If more than one lesion was present, target lesions were randomly defined for further analysis, covering a range of sizes. Per patient, all suspected PET-positive primary lesions (n = 1–3 lesions per patient) and lymph nodes (n = 0–4) and a maximum of 4 suspected PET-positive lesions in the lung (n = 0–4) or bone (n = 0–2) were chosen. An abdominal lesion was suspected in only one patient. If more than one suspected lesion was present in the lung or bone, target lesions were defined for further analysis, covering a range of sizes and subsegments of the compartments (e.g., different lung segments or bones). Size and maximum SUV of lesions were measured. The size was measured in a contrast-enhanced T1-weighted 3-dimensional fast spoiled gradient echo acquisition. Images were evaluated using the comparison protocol of an AW Workstation (version 4.5; GE Healthcare Biosciences) (*23*). The 2-reader setup was chosen to prove the reliability of semiquantitative image analyses (*24*). For the respective analysis, PET datasets were viewed in all 3 planes. The 2 readers subjectively evaluated general image quality and artifacts, image sharpness, image noise, and lesion detectability using a 4-point scale (Table 1) (*24*).

Statistical Analysis

Continuous variables were expressed as mean ± SD and categoric variables such as qualitative parameters as frequencies (percentages). For the primary lesions, the median size was calculated (1.7 cm). Lesions were subsequently defined as small when smaller than the median and as large when larger than the median. Different groups of independent samples (lesion size) were compared using the Mann–Whitney U test. Regarding qualitative parameters, we compared the

TABLE 1
Image Grading

Grade	General image quality + artifact	Image sharpness	Image noise	Lesion detectability
1	Excellent: no artifacts	Clear, excellent images	Negligible	Excellent
2	Good: some diagnostically irrelevant artifacts	Diagnostically irrelevant image blurring	Diagnostically irrelevant	Good
3	Average: diagnostically relevant artifacts	Diagnostically relevant image blurring	Diagnostically relevant	Average
4	Inadequate: marked artifacts	Inadequate image with blurring	Marked	Poor

5 reconstructions with respect to general image quality and artifacts, image sharpness, image noise, and lesion detectability using the nonparametric Friedman test for multiple samples and the Wilcoxon signed-rank test for paired samples.

Data were analyzed using commercially available software (SPSS Statistics 21, release 21.0.0; IBM). A P value of less than 0.05 indicates statistical significance.

RESULTS

Overall, 26 consecutive women with histologically proven breast cancer were analyzed (median age, 51 y; range, 34–83 y). Patients had invasive breast cancer of no special type ($n = 19$), invasive lobular breast cancer ($n = 3$), metaplastic breast cancer ($n = 2$), tubular breast cancer ($n = 1$), or cribriform breast cancer ($n = 1$). Altogether, 355 lesions (71 lesions with 5 different reconstructions) were evaluated.

There were 36 primary breast lesions (51%); 26 lesions (37%) of the axillary, hilar, or internal mammary chain lymph nodes; and 9 lesions (13%) of the bone, lung, or abdomen. Estrogen receptor α was positive in 13 (50%) of 26 patients, progesterone receptor in 16 (62%), and human epidermal growth factor receptor 2 in 9 (35%). Staging is shown in Supplemental Table 2.

An example of imaging results is shown in Figure 1.

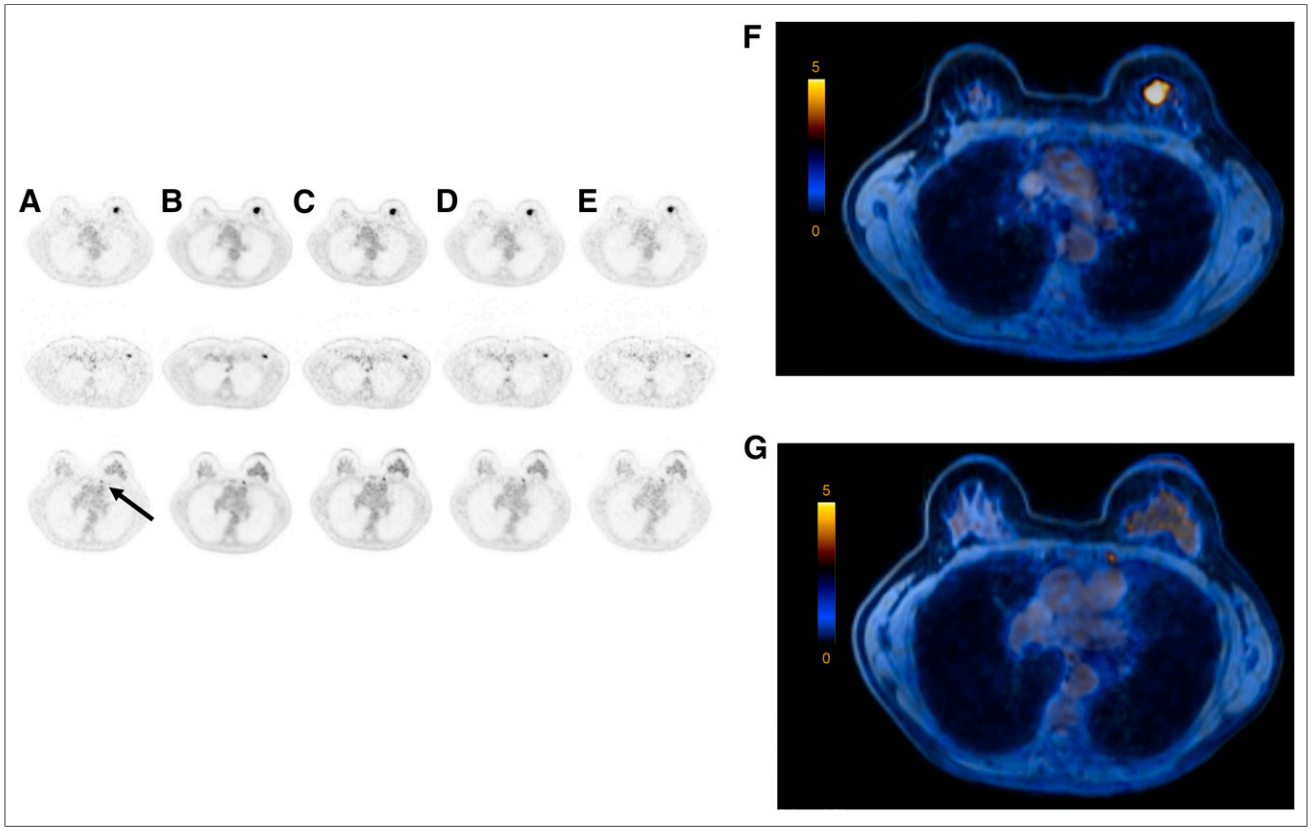

FIGURE 1. (A–E) Axial PET images of 57-y-old patient showing invasive left-sided breast cancer (top), axillary lymph node metastasis (middle), and internal mammary lymph node (bottom, arrow) after injection with 180 MBq of ^{18}F-FDG (body weight, 60 kg): 2-min TOF (A), 100% of ^{18}F-FDG dose (B), 36 MBq of ^{18}F-FDG (20% dose) (C), 18 MBq of ^{18}F-FDG (10% dose) (D), and 9 MBq of ^{18}F-FDG (5% dose) (E). For PET/MRI examination with images shown in column D, this patient would receive an estimated radiation burden of 0.36 mSv. (F and G) Axial fused PET/MR images of primary lesion (F) and internal mammary lymph node (G) (PET with 10% dose).

Image Quality and Artifacts

Rating of general image quality and artifacts showed significant differences among several reconstructions ($P < 0.001$, Friedman). General image quality and artifacts were rated best in the 20-min reconstruction with 100% dose (Table 2 for mean rating, Table 3 for comparison). Reconstructions with reduction of dose to 20% and 10% showed significantly better results than the 2-min reconstruction, and the reconstruction with a 5% dose of injected tracer was not rated as significantly different from the 2-min scan.

Image Sharpness

Rating of image sharpness showed significant differences among reconstructions ($P < 0.001$, Friedman). Image sharpness was rated best in the 20-min reconstruction with 100% dose (Table 2 for mean rating, Table 3 for comparison). Reconstructions with reduction of dose to 20% and 10% showed significantly better results than the 2-min reconstruction, and the reconstruction with a 5% dose of injected tracer was rated as significantly inferior to the 2-min scan.

Image Noise

Rating of image noise showed significant differences among reconstructions ($P < 0.001$, Friedman). Noise was rated best in the 20-min reconstruction with 100% dose (Table 2 for mean rating, Table 3 for comparison). Reconstructions with reduction of dose to 20% and 10% showed significantly better results than the 2-min reconstruction, and the reconstruction with a 5% dose of injected tracer was not rated as significantly different from the 2-min scan.

Lesion Detectability

Lesion detectability was rated as good to excellent in all reconstructions. The best results were obtained with the 20-min 100% reconstruction—significantly better than in the 2-min reconstruction (for primary lesions). The 20% and 10% reconstructions were rated as better than the 2-min reconstruction, without significant differences in primary lesions. The 5% reconstruction was rated as inferior to the 2-min reconstruction but was without significant differences in primary lesions or lymph nodes.

Lesion Size

Primary lesions (mean size, 2.0 ± 1.0 cm; range, 0.9–4.3 cm; median, 1.7 cm) were categorized as small (<1.7 cm) or large (>1.7 cm). Eight of the lesions categorized as small measured less than 1 cm. There was no significant difference in rating between small and large lesions ($P = 0.538$ for the 2-min reconstruction, $P = 0.599$ for 20 min 100%, $P = 0.753$ for 20 min 20%, $P = 1.0$ for 20 min 10%, and $P = 0.461$ for the 20 min 5%).

Calculation of Radiation Burden

The mean amount of ^{18}F-FDG injected was 225.8 ± 55 MBq (range, 179–369 MBq), resulting in an estimated whole-body radiation burden of 4.5 ± 1.1 mSv (range, 3.6–7.3 mSv) (*25*).

When 20% of the injected dose was used, a calculated mean dose of 45.2 ± 11.0 MBq (range, 35.8–73.6 MBq) would have been applied, resulting in an estimated whole-body radiation burden of 0.9 ± 0.2 mSv (range, 0.7–1.5 mSv). Similarly, when 10% of the injected dose was used, a calculated mean dose of 22.6 ± 5.5 MBq (range, 17.9–36.9 MBq) would have been applied, resulting in an estimated whole-body radiation burden of 0.5 ± 0.1 mSv (range, 0.4–0.7 mSv). When 5% of the injected dose was used, a calculated mean dose of 11.3 ± 2.8 MBq (range, 9–18.5 MBq) would have been applied, resulting in an estimated whole-body radiation burden of 0.2 ± 0.1 mSv (range, 0.2–0.4 mSv).

DISCUSSION

Our study showed that a dose reduction of up to 90% on a state-of-the-art TOF PET/MRI system with SiPM detectors for single-station imaging is feasible and produces clinically acceptable image quality.

The overall image quality in the reconstructions with a simulated dose of only 10% of the standard dose was found adequate in all measured categories, translating into a reduction of up to 90% of the injected ^{18}F-FDG dose. The image quality with 5% of the standard dose (reduction of ≤95%) was comparable to the 2-min scan currently in clinical use but had significantly inferior image sharpness. Compared with the 2-min scan currently used clinically, lesion detectability was not impaired when the dose was reduced to 5% of the clinically injected ^{18}F-FDG dose. These results indicate the possibility of a significant dose reduction in PET/MRI of suspected breast lesions. A reduction of 90% would result in an estimated effective dose of approximately 0.45 mSv for a patient weighing 75 kg (3 MBq/kg × 10/100 × 75 kg × 0.0199 mSv/MBq) (*25*). For comparison, the average effective dose for mammography, which is a widely used imaging modality for breast cancer screening, ranges from 0.44 to 0.56 mSv (*26*). This comparison is not entirely adequate, since the radiation burden in PET/MRI accounts for the whole body, whereas in mammography it is focused on a single anatomic area and the radiation burden to other organs is below 1% of the focused radiation (*27*). However, other advantages associated with lower activities are not picked up by the undersampling technique; for example, the randoms rate would be a lower proportion of the total count rate at reduced activities.

Our results show the advantage of the new technology. Attributed to the new solid-state detector design, increased axial field

TABLE 2
Image Quality Ratings

	General image quality + artifacts		Image sharpness		Image noise		Lesion detectability	
Parameter	Mean	SD	Mean	SD	Mean	SD	Mean	SD
2 min	1.84	0.6	2.28	0.6	2.16	0.6	1.46	0.7
20 min 100%	1.08	0.4	1.12	0.3	1.04	0.2	1.03	0.2
20 min 20%	1.32	0.6	1.64	0.7	1.44	0.5	1.14	0.4
20 min 10%	1.40	0.6	1.76	0.7	1.48	0.6	1.28	0.6
20 min 5%	1.88	0.5	2.60	0.8	2.28	0.5	1.62	0.8

TABLE 3
P Values for Comparison with 2-Minute Scan (Wilcoxon testing)

Parameter	General image quality + artifacts	Image sharpness	Image noise	Lesion detectability	
				Primary lesion	Lymph nodes
20 min 100%	<0.001	<0.001	<0.001	0.038	0.001
20 min 20%	<0.001	<0.001	<0.001	0.257	0.001
20 min 10%	0.001	0.001	0.001	0.763	0.032
20 min 5%	0.317	0.005	0.180	0.142	0.593

of view, and Compton scatter recovery, a significantly increased sensitivity is provided, which in turn may compensate for the dose reduction (*28*). Our results are also in line with the data of Seit et al., who investigated the effect of dose reduction in whole-body PET examinations on a PET/MRI scanner without TOF capability and lutetium oxyorthosilicate detector crystals. It was concluded that a reduction of ^{18}F-FDG of up to 33% was feasible (dose reduction to 2 MBq/kg of body weight [Biograph; Siemens]) (*29*). In a previous study by our group, we showed that when a TOF-capable PET component was used, a dose reduction of up to 50% was feasible in whole-body acquisitions in patients with normal body weight (*17*).

In the presented study, we were able to show that in single-station imaging (lesions in the breast and axilla), the injected dose could be reduced even more than in whole-body PET scans. The main reason for this reduction is obviously the imaging time for this specific bed position, which is bound to the imaging times needed for MR mammography (or any other MRI). Imaging times for MR mammography in the literature have ranged from as short as 12 min to more than 20 min. When PET detectors are kept listening throughout the entire MR mammography, significantly more counts are received than in standard whole-body imaging (usually 2–4 min/bed position). This larger number of counts, in turn, opens the opportunity to balance acquisition time versus injected dose. Another reason for the significant reduction is that suspected lesions in the breast or axillary lymph node region are relatively superficial and usually surrounded by fatty tissue or glandular breast tissue, resulting in a high signal-to-noise ratio. We suppose that results might be somewhat less impressive in single-station liver imaging, for example, in which high background noise is present. As shown in a study by Gatidis et al., clinical evaluation of image quality is in line with quantitative image metrics, and retrospective undersampling of list-mode data results in image properties equivalent to those of PET images obtained at low doses (*30*).

To date, PET imaging in oncologic examinations is restricted mainly to whole-body examinations in patients with different cancer indications. This restriction was somewhat justified by the radiation burden in the current clinical setting (5–15 mSv for a PET/CT scan). With the results of this study, this restriction might be reconsidered. Having the possibility of reducing the amount of injected tracer for specific indications will significantly reduce the radiation burden of patients, potentially resulting in a paradigm shift in PET imaging. A reduction of injected dose as presented in our results will render partial-body examinations with PET/MRI justifiable. Reduction of PET-induced radiation exposure may not only reduce possible radiation-related risks but also improve acceptance of PET among patients and referring physicians (*30*). By being opened to more indications than at present, PET/MRI might even become more economically viable (a side effect that would certainly be welcomed). One specific example is the work-up of Breast Imaging Reporting and Data System 3 lesions. These lesions cannot be sufficiently classified and therefore usually need follow-up. Work-up of such lesions with a rather low probability of malignancy requires techniques with low (or no) radiation exposure, to achieve an acceptable risk–benefit ratio. MRI is partly used for this indication but has certain limitations. Also, those lesions may occur in younger patients, who are at higher risk for developing radiation-induced diseases. PET/MRI has the potential to characterize multiparametric qualitative and quantitative features and therefore can improve tumor characterization and outcome prediction (*31*). Also, PET/MRI has already been shown useful in whole-body staging of patients with invasive ductal breast carcinoma and recurrent breast cancer (*11,14,32*). The potential for highly accurate characterization of breast lesions using PET techniques has been demonstrated by Yamamoto et al. (*16*). In a screening setting with 265 women, those authors were able to show that abnormal ^{18}F-FDG uptake (detected with PEM) showed a sensitivity of 100% and a specificity of 84.5%. In their study, PET imaging showed a detection rate of 2.3%, which is higher than the reported detection rate of mammography and physical examination (0.31%) but may be partly explained by a selection bias in their study. The authors concluded that the detection of abnormal ^{18}F-FDG uptake had potential for breast cancer screening. PEM offers the possibility of better image quality for breast lesions, since the detectors are closer to the lesions, resulting in a higher spatial resolution. However, no study has compared the sensitivity of PEM with that of the newly available SiPM-detector PET systems, which have a high sensitivity but are obviously not as close to the breast tissue as within a PEM system. PEM systems are not widely available and still fail to be considered a useful adjunct to MRI in clinical imaging, despite promising initial results (*16,33,34*).

The results of our study are not necessarily restricted to imaging with ^{18}F-FDG. Currently, there are several receptor-specific tracers under investigation, and these offer potential beyond the capabilities of current clinical imaging. For example, there is 16α-^{18}F-fluoro-17β-estradiol, a fluorinated estradiol targeting the estrogen receptor; radionuclides targeting human epidermal growth factor receptor 2; somatostatin receptor–mediated imaging; and gastrin-releasing peptide receptor imaging, which could be applied for disease characterization, staging, or monitoring of therapy response (*35*). However, those research questions have to be investigated separately.

Our study had several limitations. The results were limited to the breast and axillary regions. These regions have a higher signal-to-noise ratio, since there is a lot of adipose tissue with low ^{18}F-FDG

avidity. Other indications, such as for assessment of suspected liver lesions, should be investigated in further studies. In the present study, only 3 (12%) of our 26 patients had a body mass index above 30. In obese patients, higher injected doses are expected to be needed for adequate image quality. We included only patients with biopsy-proven breast cancer lesions who underwent whole-body PET/CT. Therefore, and because there is a certain patient selection bias in our population toward more aggressive breast cancer types, our study does not allow us to draw a conclusion on the extent to which uptake of ^{18}F-FDG might contribute to the diagnostic work-up of suspected (but not yet proven) malignant breast lesions. However, this topic has been addressed in several previous studies with promising results (*34*).

CONCLUSION

PET detectors with SiPM and TOF capability offer high-quality imaging using a single-station PET/MRI scanner. A reduction of up to 90% of the currently clinically used injected dose of ^{18}F-FDG was found to be adequate for single-station breast imaging. The calculated radiation exposure would be comparable to the effective dose of a single digital mammogram. A reduction of radiation burden to this level might render partial-body examinations with PET/MRI justifiable.

DISCLOSURE

Patrick Veit-Haibach received investigator-initiated study grants from Bayer Healthcare, Siemens Healthcare, Roche Pharmaceuticals, and GE Healthcare and speaker's fees from GE Healthcare. Tetsuro Sekine received investigator-initiated study grants from the Hitachi Global Foundation and the Fukuda Foundation for Medical Technology. Bert-Ram Sah received a research grant from the Swiss National Science Foundation. The Department of Nuclear Medicine holds an institutional grant from GE Healthcare. No other potential conflict of interest relevant to this article was reported.

ACKNOWLEDGMENTS

We thank the technologists at the University Hospital of Zurich for their help in acquiring the data and freeing up resources.

REFERENCES

1. Hess S, Blomberg BA, Zhu HJ, Hoilund-Carlsen PF, Alavi A. The pivotal role of FDG-PET/CT in modern medicine. *Acad Radiol.* 2014;21:232–249.
2. Sheikhbahaei S, Mena E, Pattanayak P, Taghipour M, Solnes LB, Subramaniam RM. Molecular imaging and precision medicine: PET/computed tomography and therapy response assessment in oncology. *PET Clin.* 2017;12:105–118.
3. Townsend DW. Dual-modality imaging: combining anatomy and function. *J Nucl Med.* 2008;49:938–955.
4. Muzic RF Jr, DiFilippo FP. Positron emission tomography-magnetic resonance imaging: technical review. *Semin Roentgenol.* 2014;49:242–254.
5. Kiser J. Molecular imaging and its role in the management of breast cancer. *Clin Obstet Gynecol.* 2016;59:403–411.
6. Giess CS, Chikarmane SA, Sippo DA, Birdwell RL. Breast MR imaging for equivocal mammographic findings: help or hindrance? *Radiographics.* 2016;36:943–956.
7. Bychkovsky BL, Lin NU. Imaging in the evaluation and follow-up of early and advanced breast cancer: when, why, and how often? *Breast.* 2017;31:318–324.
8. Berg WA. Nuclear breast imaging: clinical results and future directions. *J Nucl Med.* 2016;57(suppl 1):46S–52S.
9. Melsaether A, Moy L. Breast PET/MR imaging. *Radiol Clin North Am.* 2017;55:579–589.
10. Rice SL, Friedman KP. Clinical PET-MR imaging in breast cancer and lung cancer. *PET Clin.* 2016;11:387–402.
11. Sawicki LM, Grueneisen J, Schaarschmidt BM, et al. Evaluation of ^{18}F-FDG PET/MRI, ^{18}F-FDG PET/CT, MRI, and CT in whole-body staging of recurrent breast cancer. *Eur J Radiol.* 2016;85:459–465.
12. Gillies RJ, Beyer T. PET and MRI: is the whole greater than the sum of its parts? *Cancer Res.* 2016;76:6163–6166.
13. Melsaether AN, Raad RA, Pujara AC, et al. Comparison of whole-body ^{18}F FDG PET/MR imaging and whole-body ^{18}F FDG PET/CT in terms of lesion detection and radiation dose in patients with breast cancer. *Radiology.* 2016;281:193–202.
14. Grueneisen J, Sawicki LM, Wetter A, et al. Evaluation of PET and MR datasets in integrated ^{18}F-FDG PET/MRI: a comparison of different MR sequences for whole-body restaging of breast cancer patients. *Eur J Radiol.* 2017;89:14–19.
15. Kuhl CK. The changing world of breast cancer: a radiologist's perspective. *Plast Surg Nurs.* 2016;36:31–49.
16. Yamamoto Y, Tasaki Y, Kuwada Y, Ozawa Y, Inoue T. A preliminary report of breast cancer screening by positron emission mammography. *Ann Nucl Med.* 2016;30:130–137.
17. Sekine T, Delso G, Zeimpekis KG, et al. Reduction of ^{18}F-FDG dose in clinical PET/MR imaging by using silicon photomultiplier detectors. *Radiology.* 2017;286:249–259.
18. Herzog H, Lerche C. Advances in clinical PET/MRI instrumentation. *PET Clin.* 2016;11:95–103.
19. Queiroz MA, Delso G, Wollenweber S, et al. Dose optimization in TOF-PET/MR compared to TOF-PET/CT. *PLoS One.* 2015;10:e0128842.
20. Zeimpekis KG, Barbosa F, Hullner M, et al. Clinical evaluation of PET image quality as a function of acquisition time in a new TOF-PET/MRI compared to TOF-PET/CT: initial results. *Mol Imaging Biol.* 2015;17:735–744.
21. Ter Voert EE, Delso G, de Galiza Barbosa F, Huellner M, Veit-Haibach P. The effect of defective PET detectors in clinical simultaneous [^{18}F]FDG time-of-flight PET/MR imaging. *Mol Imaging Biol.* 2017;19:626–635.
22. Levin CGG, Deller T, McDaniel DL, Peterson W, Maramraju SH. Prototype time-of-flight PET ring integrated with a 3T MRI system for simultaneous whole-body PET/MR imaging [abstract]. *J Nucl Med.* 2013;54(suppl 2):148.
23. Sah BR, Stolzmann P, Delso G, et al. Clinical evaluation of a block sequential regularized expectation maximization reconstruction algorithm in ^{18}F-FDG PET/CT studies. *Nucl Med Commun.* 2017;38:57–66.
24. Stansfield EC, Sheehy N, Zurakowski D, Vija AH, Fahey FH, Treves ST. Pediatric ^{99m}Tc-MDP bone SPECT with ordered subset expectation maximization iterative reconstruction with isotropic 3D resolution recovery. *Radiology.* 2010;257:793–801.
25. Quinn B, Dauer Z, Pandit-Taskar N, Schoder H, Dauer LT. Radiation dosimetry of ^{18}F-FDG PET/CT: incorporating exam-specific parameters in dose estimates. *BMC Med Imaging.* 2016;16:41.
26. Hendrick RE. Radiation doses and cancer risks from breast imaging studies. *Radiology.* 2010;257:246–253.
27. Sechopoulos I, Suryanarayanan S, Vedantham S, D'Orsi CJ, Karellas A. Radiation dose to organs and tissues from mammography: Monte Carlo and phantom study. *Radiology.* 2008;246:434–443.
28. Grant AM, Deller TW, Khalighi MM, Maramraju SH, Delso G, Levin CS. NEMA NU 2-2012 performance studies for the SiPM-based ToF-PET component of the GE SIGNA PET/MR system. *Med Phys.* 2016;43:2334.
29. Seith F, Schmidt H, Kunz J, et al. Simulation of tracer dose reduction in ^{18}F-FDG PET/MRI: effects on oncologic reading, image quality, and artifacts. *J Nucl Med.* 2017;58:1699–1705.
30. Gatidis S, Wurslin C, Seith F, et al. Towards tracer dose reduction in PET studies: simulation of dose reduction by retrospective randomized undersampling of list-mode data. *Hell J Nucl Med.* 2016;19:15–18.
31. Plecha DM, Faulhaber P. PET/MRI of the breast. *Eur J Radiol.* 2017;94:A26–A34.
32. Catalano OA, Daye D, Signore A, et al. Staging performance of whole-body DWI, PET/CT and PET/MRI in invasive ductal carcinoma of the breast. *Int J Oncol.* 2017;51:281–288.
33. Tafra L, Cheng Z, Uddo J, et al. Pilot clinical trial of ^{18}F-fluorodeoxyglucose positron-emission mammography in the surgical management of breast cancer. *Am J Surg.* 2005;190:628–632.
34. Bitencourt AG, Lima EN, Macedo BR, Conrado JL, Marques EF, Chojniak R. Can positron emission mammography help to identify clinically significant breast cancer in women with suspicious calcifications on mammography? *Eur Radiol.* 2017;27:1893–1900.
35. Dalm SU, Verzijlbergen JF, De Jong M. Review: receptor targeted nuclear imaging of breast cancer. *Int J Mol Sci.* 2017;18:E260.